TURBULENCE RECOGNITION IN FREE CONVECTIVE FLOW BY THERMAL-VIDEO POST-PROCESSING IN THE CASE OF A THERMAL POWER PLANT MILL

by

Suzana Lj. LINIĆ[a*], Mihajlo S. LINIĆ[b], Bojana M. RADOJKOVIĆ[c], Slavica S. RISTIĆ[d], and Bore V. JEGDIĆ[c]

[a] Innovation Center, Faculty of Mechanical Engineering, University of Belgrade, Belgrade, Serbia
[b] Faculty of Electrical Engineering, University of Belgrade, Belgrade, Serbia
[c] Institute of Chemistry, Technology and Metallurgy, University of Belgrade, Belgrade, Serbia
[d] Central Institute for Conservation, Belgrade, Serbia

Original scientific paper
https://doi.org/10.2298/TSCI200907341L

This paper presents a study of a free convection flow around the walls of a ventilation mill of the Thermal Power Plant "Kostolac B", Kostolac, Serbia. A combined method consists of thermography and software post-processing, PATS. The PATS is specially developed for recognition of turbulence zones by the custom processing of large input data sets from thermal videos. The calculations determine maximum temperature fluctuation i.e. peak-to-peak fluctuation at every spot during the recording time. Three thermal videos of the walls were analyzed. Maximum temperature fluctuation occurred in the zones close to the obstacles, which are thus recognized as one of the main sources of turbulence. Besides, PATS has recognized fine camera oscillations and mechanical movements of a flexible material near the dozer wall. The detected zones of turbulence correspond to the previous studies and to the theory. The method shows good potential in the field of free convective flow research through the improvement of testing efficiency and cost savings. State-of-the-art thermograph cameras and updated software are recommended.

Key words: *convection, turbulence, thermography, post-processing*

Introduction

Many studies were dedicated to free convective flow, its mechanism of appearance, and the behavior of the boundary-layer around heated objects, mostly to improve the knowledge base and apply it to industrial problems or to environmental protection. Even from the basics of free convective flow and the history of its research, one may note its complex nature, which thus leads to mainly empirical, still evolving solutions [1-3]. Free convective flow exists when the temperature field in a fluid is non-uniform, *i.e.* temperature gradients produce density gradients, and when gravity or other mass forces such as centrifugal, Coriolis, electromagnetic forces, *etc.* generate the fluid motion Martynenko *et al.* [4]. In theory, free convective flow and heat transfer are represented by fundamental equations of conservation of momentum, mass, and energy, involving the inertial forces. Heat transfer depends on the object shape and the configuration of its wetted surfaces, temperature distribution, temperature

* Corresponding author, e-mail: slinic@mas.bg.ac.rs

fluctuations, and thermophysical properties of the fluid. The analytical solutions are approximated and confirmed with the experimentally obtained results. The Boussinesq approximation Martynenko *et al.* [4] has been introduced under the assumptions of a steady 2-D and laminar flow driven by buoyancy forces and involving difference in density. The flow over a vertical heated wall exists inside a thin velocity boundary-layer. The temperature distribution across the flow defines the thermal boundary-layer. Hence, depending on the conditions and the object topology, the flow may behave as laminar, transitional, or turbulent. The laminar boundary-layer under some external conditions may be disturbed initially, than it gradually develops downstream, where the flow loses its stability and transforms into a transitional, and, further on, into a turbulent flow. The initiation and development of turbulence in a free convective flow are much more different from the mechanism occurring in a forced convection flow White [5]. The sources of disturbances, as reported in Martynenko *et al.* [4], might be an unstable heat source, vibrations of the facility, instabilities of the environmental conditions, *etc.*

Turbulent free convective flows have been studied using reliable numerical simulations, which can shed light on some of hardly recognizable parameters. For example, in Zhao *et al.* [6], different temperature frequency profiles of laminar, transient, and turbulent flows were studied. However, experimental work is irreplaceable and it is nowadays applied alongside numerical simulations for a more detailed insight. Due to the specific flow characteristics of a free convective flow, different flow parameters such as velocity, temperature, and field of the heat flux have to be simultaneously measured *i.e.* recorded in accordance with their coupled existence in the field. The wind tunnel testing techniques for measuring velocity and temperature in a turbulent flow mainly apply hot-wires and thermocouples Ristić *et al.* [7]. However, in the case of a specific free convection flow, the construction of hot-wires and other equipment has to be adapted to the purpose [8, 9]. A special difficulty in measurements is capturing realistic flow unsteadiness. The tools for advanced quantitative and qualitative analyses, *i.e.* non-destructive optical methods such as shadowgraph, laser Doppler anemometry, classical or holographic interferometry, and particle image velocimetry [7] are capable of visualizing the flow field. Unfortunately, the methods such as shadowgraph and interferometry require a sufficient density difference in the flow. A common characteristic of all the mentioned methods is that they are hard to apply out of laboratory conditions. Furthermore, as reported in De Larochelambert [9], a special, challenging case is a highly heated vertical wall when the turbulent flow behaves differently, creating coherent structures in the flow.

In the last three or more decades, infrared thermography (IRT) has been introduced to wind-tunnel tests for boundary-layer studies in a forced convective flow to improve testing efficiency and cost savings. The IRT is able to trace the zone of transitional flow on the basis on temperature difference [10-12] and temperature measurements on surfaces of large dimensions. Its advantage is in imaging (both of a single image or a series of images) ordered in the time history, t, in the form of thermal videos from various angles. This is illustrated by the IRT observations of the boundary-layer transition over a standard model of the flat plate heated with different heating techniques presented in Simon *et al.* [12]. The flow characterization was investigated over a simplified high speed train model in a low-speed wind tunnel using thermography, oil-emulsion visualization, and numerical simulations Linić *et al.* [13]. The IRT is nowadays an experimentally justified, valuable, and affordable method, as well as an efficient one, especially in the phase of concept design or pre-testing in boundary-layer studies.

In industrial facilities such as thermal power plants, monitoring of the thermal status is necessary to maintain their functional efficiency. The surface temperature of the ventilation mill (VM) walls depends on the working temperature of the multiphase mixture (pulverized

coal, recirculation gases, and impurity particles such as sand) inside the mill, the insulation condition, and the ambient temperature. The aim of the initial investigations was to detect the positions of the insulation damage using IRT. Extensive investigations of the VM at the thermal power plant (TPP) "Kostolac B", Kostolac, Serbia, were conducted by numerical simulations and IRT in order to improve functional efficiency [14, 15]. The potential of IRT for turbulence recognition became clearer when the analysis was extended to include the extreme surface temperature differences noticed from thermal videos. The maximum surface temperature deviations over time have been analyzed manually for several selected measuring lines (1 pixel wide) in Linić *et al.* [16]. The method has shown that the highest deviations in maximum temperatures on the observed surfaces occur around obstacles, as expected from the theory. However, the application of this method was time-consuming.

In this study, a set of previous records [16, 17] has been used to contribute to the knowledge of IRT application in the field of free convective flow investigations. Already confirmed as a valuable tool for monitoring the VM operation and the insulation conditions, IRT was also implemented here as a pre-testing measurement method. Its task was to easily determine the region of interest in the boundary-layer at which a measuring device (*e.g.* a hot-wire or a thermocouple) has to be introduced for more precise results. The method is not just aimed to be applied to the VM but also to similar cases for recognizing a turbulent flow (radiators, heat exchangers, *etc.*). There are no standard software tools for analyzing the boundary-layer in a free convective flow by thermography. Therefore, for time- and cost-efficient testing, a custom code for analyzing large sets of IRT recorded data was proven necessary. The custom code was set as a specific goal of this research realized by PATS software. It is certain that the future work will improve the experiences and knowledge in the field, especially if high resolution and high speed IRT cameras are to be used. The obtained results may indicate in practice, for example, places with local high turbulence but also places with poor sealing. Such occurrences have a negative effect on energy efficiency, wall structures, and environmental protection.

Methods

Experimental method

One of eight VM of the lignite TPP "Kostolac B", Block 2, was selected for this study. The available nominal capacity of the Blocks B1 and B2, generating about 303 MWh of electric power, is 640 MW in total (320 MW per unit). Figure 1 shows the left and the front side set-up for the recording of the selected VM No. 6 with the main parts and the highlighted zones of interest for this work. The prepared coal mass, with impurities like sand and mineral particles, enters the VM from the dozer. The VM is continually fed with the coal mass heated by air (≈ 250 ºC) Kozić *et al.* [14], through the front inlet located in the rotor center. The VM is of EVT N 270.45 type (nominal capacity ≈ 76 ton per hour of coal). The grinding wheel (3.6 m in diameter) with impact plates captures the coal mass, accelerates it by rotation (420-500 rpm), while drying and shredding it partially. The main grinding process occurs by collision of coal lumps and the fixed impact plate, at the top of the VM, at their nearest interior distance. The process of coal pulverization produces fine particles of coal (average size 150 μm in diameter). Pulverized coal, carried by a re-circulation gas, forms a lifting stream ($\overline{T}_{\text{exit}}$ = 168 ºC) Kozić *et al.* [14] at the VM exit. The mixture is directed upwards, to the channel with separators, directly to the system of four-level burners. In this way, the tangential firing provides efficient and stable combustion of pulverized coal

in boiler furnace. This firing method providing complete fuel combustion and uniform heat distribution inside the furnace.

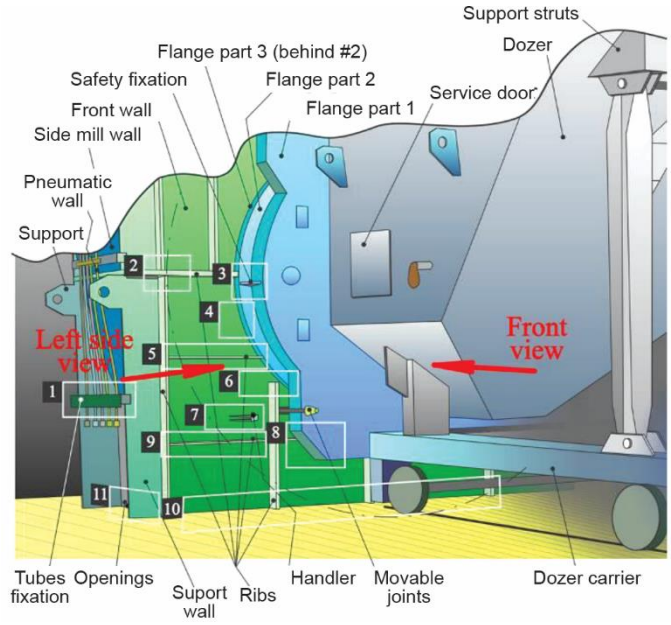

Figure 1. Illustration of the set-up

The basic purpose of the measurements was to record the temperature distribution on the walls of the VM housing at the TPP "Kostolac B" after its insulation had been repaired Linić *et al.* [17]. A large set of overlapped thermal video records (TVR) was made to record temperatures over the VM6 with the highest possible quality.

For turbulence recognition, as the main goal of the present study, three TVR were selected. Test 1 was recorded from the left side during $t_1 \approx 22$ seconds. Test 2 from the right side, $t_2 \approx 4$ seconds. Test 3 from the front side of the VM 6, $t_3 \approx 3$ seconds. The industrial thermal camera FLIR E40 SC was used (with a temperature range from 0 °C to 650 °C, minimum temperature difference detectable outside the signal noise range *i.e.* thermal sensitivity < 0.07 °C at 30 °C, and a frame rate of $f = 30$ fps). It was controlled with FLIR Research software. During a single grinding wheel rotation, about 4.3 to 3.6 frames were recorded. The FLIR Research software and FLIR Tools were used for the basic TVR analysis with options of exporting the files (.csv). These files consist of the set-up data: the spot positions on the image ($x \times y = 320$ px × 240 px), and the surface temperatures per spot per frame (the spot is an image surface of the dimensions 1 px × 1 px).

Method of analysis

The IRT method is a non-destructive method of measuring surface temperatures, suitable for complex topologies. It is expected to recognize the fluctuations in temperature representing turbulences on walls and over complex surfaces with steps, ribs, cylinders, *etc.*, fig. 2 [1-4].

Since thermal imaging results are dependent on the ambient influences (atmosphere absorption, near-objects reflections), surface characteristics (emissivity, roughness, *etc.*), and

support steadiness, a careful camera set-up is necessary. Figure 3(a) describes the method of analysis at an arbitrary spot M.

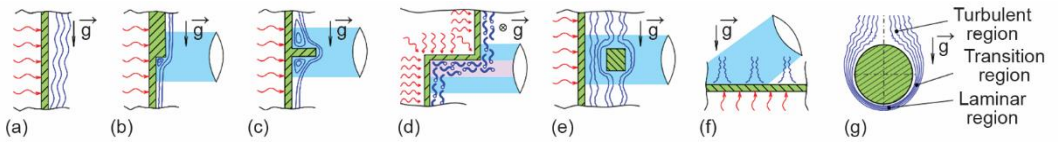

Figure 2. Free convective flow cases around different surface topologies

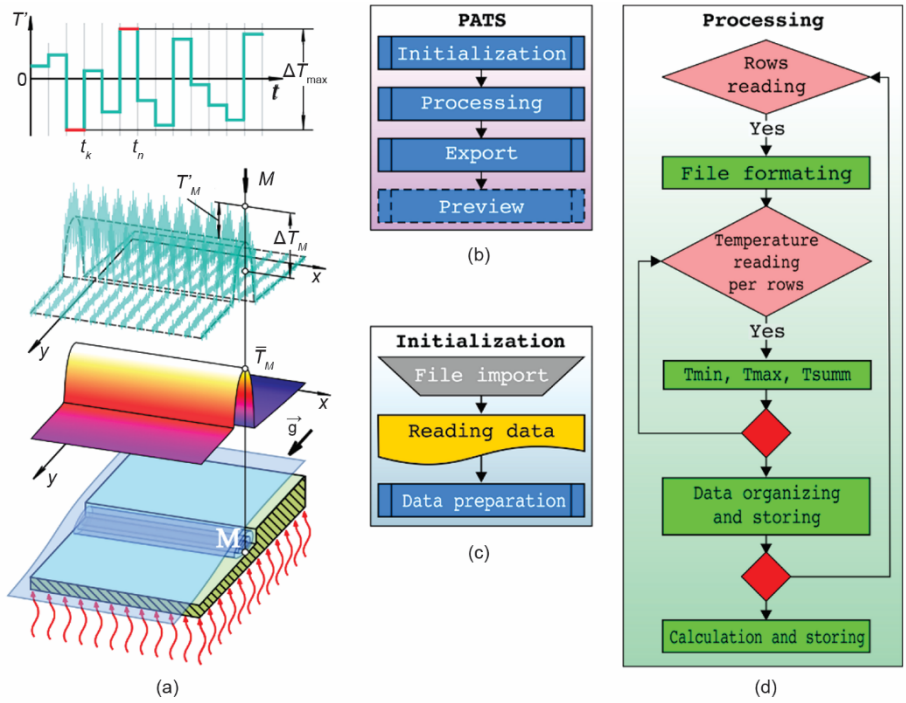

Figure 3. Analysis method and the main structure of the PATS algorithm for the post-processing of a TVR

As shown in fig. 3(a), the spot temperature, T recorded in time, is expressed as a sum of the time-averaged spot temperature, $\overline{T}$, and the spot temperature fluctuating component, T', analogous to the description of forced convection in the compressible flow [18]. A true, realistic representation of T fluctuation is found in the map consisting of the maximum spot temperature changes, ΔT_{max}, and representing peak-to-peak temperature fluctuations occurring over individual TVR durations. One may note that the values on the ΔT_{max} map are related to different moments (t_k and t_n at the spot M), fig. 3(a). Independency of $\overline{T}$ from time is obtained by the prolongation of the recording time, while T' is preferred to be monitored by a high resolution and high speed thermal camera. However, even though the industrial class of cameras is used, a huge amount of collected data requires automated processing for analysis (for example, the input file of Test 1 has n = 683 frames and each frame contains 320 × 240 spot temperature data, counting 52.454.400 data for processing).

The PATS post-processing software has been coded with the purpose of custom analysis of the large set of data collected by TVR for turbulence recognition over the VM6 surfaces [19]. The main advantage of PATS is that turbulence is recognized based upon the maximum temperature fluctuation range, peak-to-peak, in the TVR time. On the contrary, manual analyses have recognized turbulence due to selected local T_{max}, [16]. The post-processing is applicable after TVR. The set-up and measurement quality may be corrected in re-recording, and it is comfortable for use both with industrial and research thermal cameras. The open source software C#, of the open source platform Visual Studio 2017, has been applied for coding PATS [20].

The main structure of the PATS algorithm is composed of the following processes: initialization, processing, export, and, optionally, a result preview, fig. 3(b). The initialization starts PATS, searches, and imports the .csv data (created with the standard FLIR TOOLS software) for processing, fig. 3(c). The number of spots in the rows and the columns is calculated from the first TVR frame. The number of frames, n, recorded in TVR is calculated based on the repeated keyword in the file. Both n and f, together, serve to determine the recording time. The dedicated structure serves the organized filling of files with data at each spot through the TVR as follows: the minimum spot temperature T_{min} and T_{max}, the maximum spot temperature, the sum of spot temperatures during TVR and the spot temperature difference over time, ΔT_{max}, necessary for data sorting. The data are organized in a 2-D matrix in accordance with the positions of spots and further stored.

The processing consists of two phases illustrated in fig. 3(d). The first phase reads data through rows in loops. The second processing phase starts with the calculation of ΔT_{max}, per spot from the mean value, in the time history. Ordered in the matrix, data are exported to readable formatted textual files. The open source software GNUPLOT Williams *et al.* [21] is selected to visualize large data files.

Results and discussion

The first set of the results from Tests 1-3 contains the overlapped maps of T (first frame, FLIR Research), ΔT_{max}, PATS [19], with the highlighted extremes of ΔT_{max} (points A-D, PATS), and the separate selected individual $T(t)$ diagrams (points P1-P15), shown in figs. 4(a), 5(a), and 6(a), respectively. For a better insight, the intervals of ΔT_{max} signed on the color bar with the cross are removed from the maps. The other set of results represents $T'(t)$ at five spots (No. 1-5), [19]. These spots present the first five calculated ΔT_{max} extremes, figs. 4(b), 5(b), and 6(b), respectively. The respective legend contains the spot position data (with the noted spot A) and the corresponding values ΔT_{max}, T_{max}, T_{min}, and $\overline{T}$, defined by PATS.

From fig. 4(a), it is interpreted that the most intensive turbulence in Test 1 occurred at the spot A, zone 1, ΔT_{max} = 15.624 ºC, with the largest $\overline{T}$ in the list, where the record captured both the turbulence over the sidewall and that around the bar, a case such as one in fig. 2(e). The second and single-spot ΔT_{max} peak is placed at zone 5 under the rib, fig. 4(b) No. 2. Furthermore, the most intensive changes of $T(t)$ are noticed at the spots P1, P4, and ΔT_{max} values at zones 2, 5, 7, and 9, in fig. 4(a), which was interpreted as turbulence created over different obstacles. At the spots P2 and P3, turbulence is recognized over the curved surfaces of the flanges. As the bottom part of the VM is built in the concrete floor, heat is transferred to the concrete floor by conduction. The point P5 is positioned on the floor and the flow at this point was characterized as turbulent, in accordance with the $T(t)$ range of ≈ 0.5 ºC over the recording time, fig. 4(a).

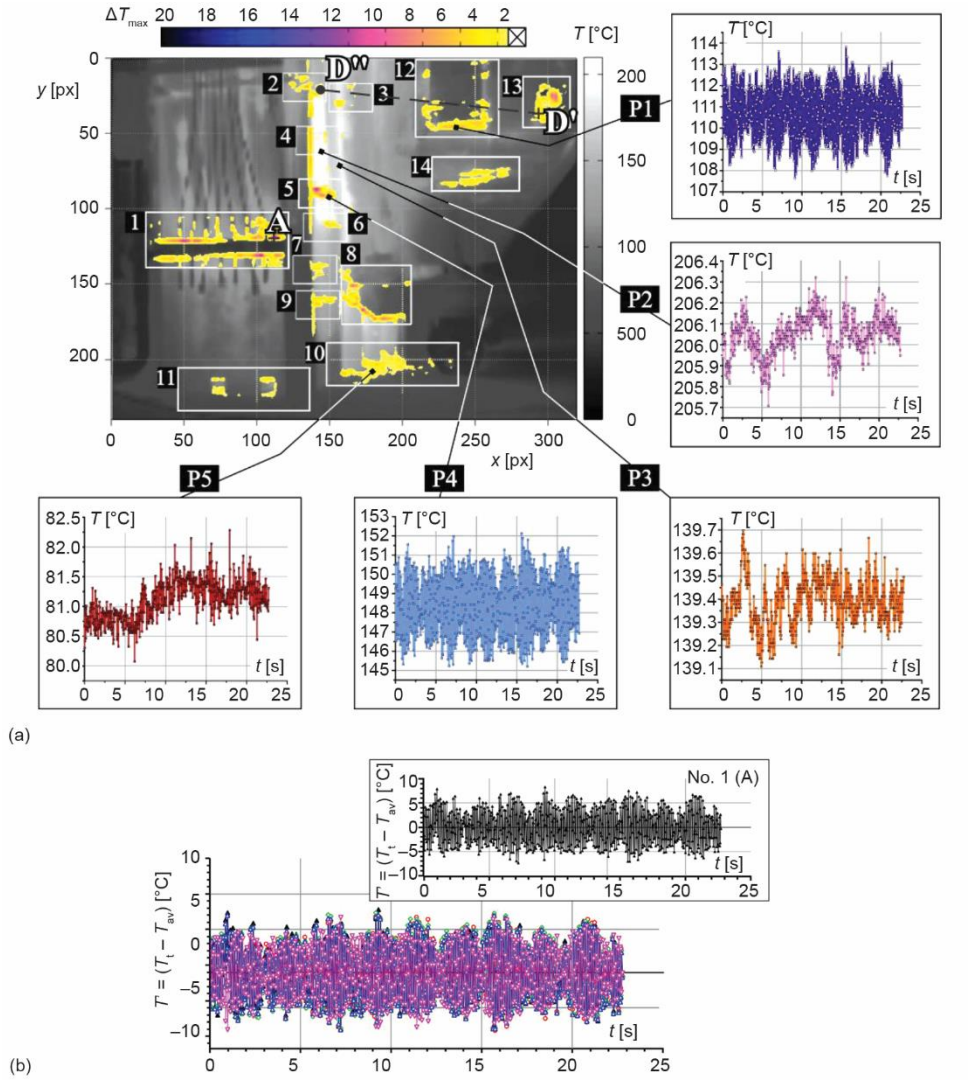

Legend

	No.	x [px]	y [px]	ΔT_{max} [ºC]	T_{max} [ºC]	T_{min} [ºC]	$\bar{T}$ [ºC]
▲	1 (A)	110	118	15.624	97.86	82.236	90.497
○	2	140	86	15.378	160.039	144.661	152.383
◇	3	112	118	15.19	90.689	75.499	83.345
△	4	111	118	15.029	94.301	79.272	86.954
▽	5	102	130	14.715	90.004	75.286	82.515

Figure 4. Combined results from Test 1 (the left side of the VM); (a) overlapped maps of T and ΔT_{max} [19] with the diagrams of the $T(t)$ at the points P1-P5, and (b) curves $T'(t)$ at the spots with the five highest ΔT_{max} [19]

The turbulence recognized over the flange surfaces shows the potentials of IRT in this kind of testing. Further investigations from the closer view recorded with an advanced IRT device and controlled conditions are needed to try to recognize changes in potentially coherent structures of the boundary-layer as reported in De Larochelambert [9]. The $T(t)$ at the point P3, from fig. 4(b), suggested that the flow is turbulent but in a close range of about 0.6 ºC. Further observations from a close distance, flow visualization, and temperature-velocity tests are recommended for more precise results. The distinctive values of $T'(t)$ are recognized near the obstacles and their intensity is rather related to the shape and dimensions (the rib thickness is 20 mm, its length is about 100 mm) than to the local $\bar{T}$ or T_{max}, fig. 4(b) (similarly to the fig. 2 cases). The spots with ΔT_{max}, have not given the five displaced unique peaks over the map, but rather the neighboring to the local maximum, thus the additional quarries have to be implemented in the PATS updated version to accomplish this requirement.

In Test 2, the largest ΔT_{max} is recognized near the cylindrical cover on the flange, B, and around the leader bar, C, fig. 5(a). A type of cyclic change of $T'(t)$ is recognized at B and C, fig. 5(b), which together with $T(t)$ at the points P6, P8, and P9 have shown minimum magnitude occurring after about $t \approx 1$ second, fig. 5(a). In this case, the similarity of $T'(t)$ behavior at B and C is interpreted as the presence of combined turbulence and the influence of fine vibrations of the IRT camera.

On the map in fig. 6(a), the range of $\Delta T_{max} < 4$ °C is intentionally selected to present only those results which are related to turbulence, according to the analysis. An actual value, shown in fig. 6(b), is $\Delta T_{max} = 20.146$ °C, but it may mislead the analysis if it is not performed with care.

As expected, the largest ΔT_{max} values, shown in fig. 6(a), are related to the spots near different obstacles and over the side surfaces of the flange. In the zone B' (the position near B in fig. 5(a), from the front view) the distinctive ΔT_{max} is present. One may note that the dozer, in the center of the map, fig. 6(a), has its boundary-layer, which is obstructing the recording in the zone of the flange in the front view because it presents the local atmosphere with undefined characteristics, similar to that shown in fig. 2(d). In fig. 6(a), three objects arranged in depth are captured – the first one is the plane of VM6 front, the next one is the long and inclined surface of the dozer, and the last one, closest to the thermal camera, is the strut, fig. 1. Since the IRT camera set-up data are set to the VM6 front, other readings on the map may be questionable and as such are not discussed here. The distinctive ΔT_{max} values are related to the flow over the ribs (P13), the cylindrical cover (B', P12), the wall surfaces (P14, P15), and the sides of the flange (P11). The removed values from the map are in the range of $\Delta T_{max} = 4$-20 °C and they are placed in the close zone of the point D, figs. 6(a) and 6(b). The represented changes of $T'(t)$, fig. 6(b), originated from the mechanical movements of the free-hanging end of a flexible material that temporarily wadded the pipe at the dozer side. The swinging of the free-hanging end produced a large temperature difference at the measuring spots, which is hardly recognized without PATS, depending on the currently captured target, a colder object – flexible material or the surface of the hot VM6 front. Nevertheless, the unexpected test results were useful to visualize the local influence of the boundary-layer around the dozer on the basis of swinging of the flexible material.

The results from Test 3 have shown that the ΔT_{max} map $T'(t)$ analysis, determined with PATS, suggests that those may be used as representative parameters for recognizing turbulence in a free convective flow, especially over various obstacles. The results are in agreement with the manually processed results in [16], showing a higher precision, and with the theory. In the tests presented in this work, an industrial camera was used but, for more precise

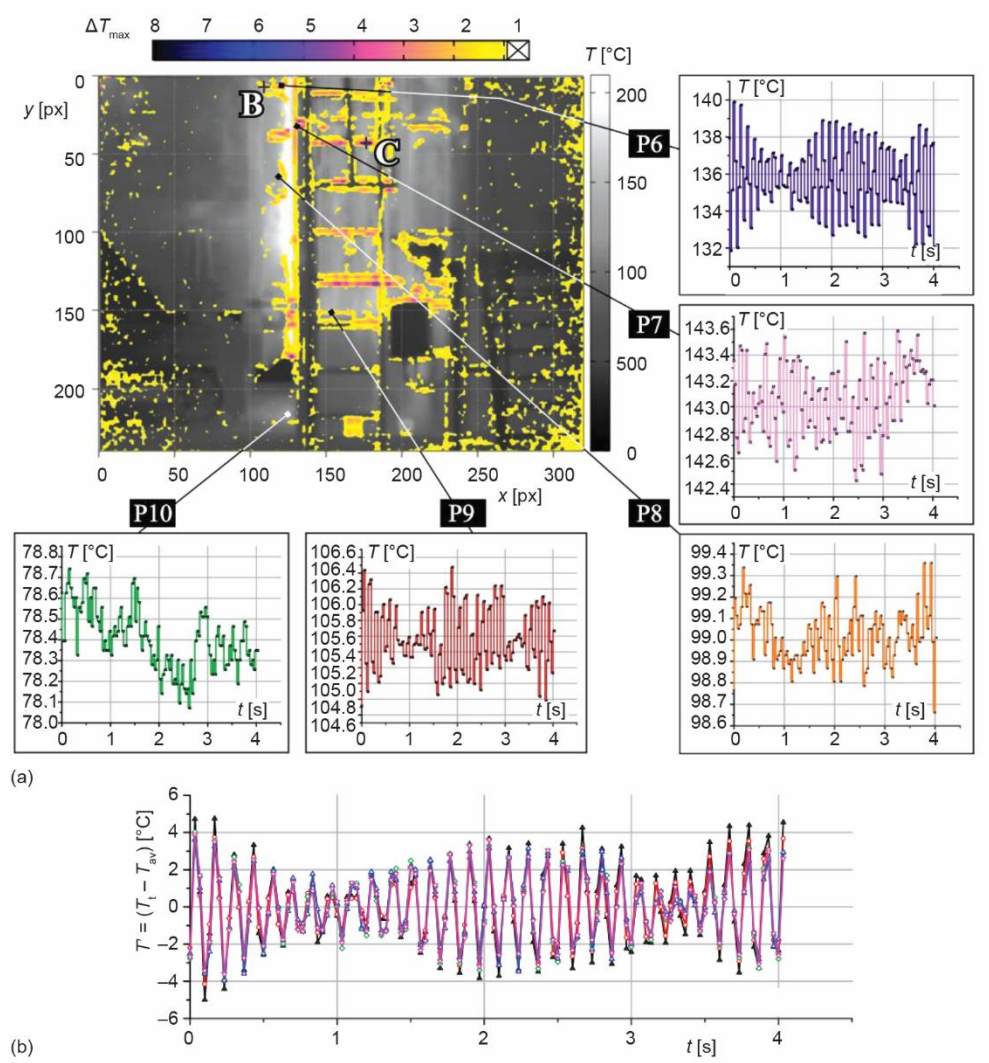

Legend

	No.	x [px]	y [px]	ΔT_{max} [ºC]	T_{max} [ºC]	T_{min} [ºC]	$\bar{T}$ [ºC]
	1(B)	120	6	9.747	168.775	159.028	163.776
	2	119	6	8.039	139.901	131.862	135.746
	3(C)	176	42	7.953	82.078	74.125	78.149
	4	108	6	7.569	110.371	102801	106.421
	5	175	42	7.515	81.33	73.815	77.719

Figure 5. Combined results from Test 2 (the right side); (a) overlapped maps of T and ΔT_{max} [19] with the diagrams of the $T(t)$ at the points P6-P10 and (b) burves $T'(t)$ at the spots with the five highest ΔT_{max} [19]

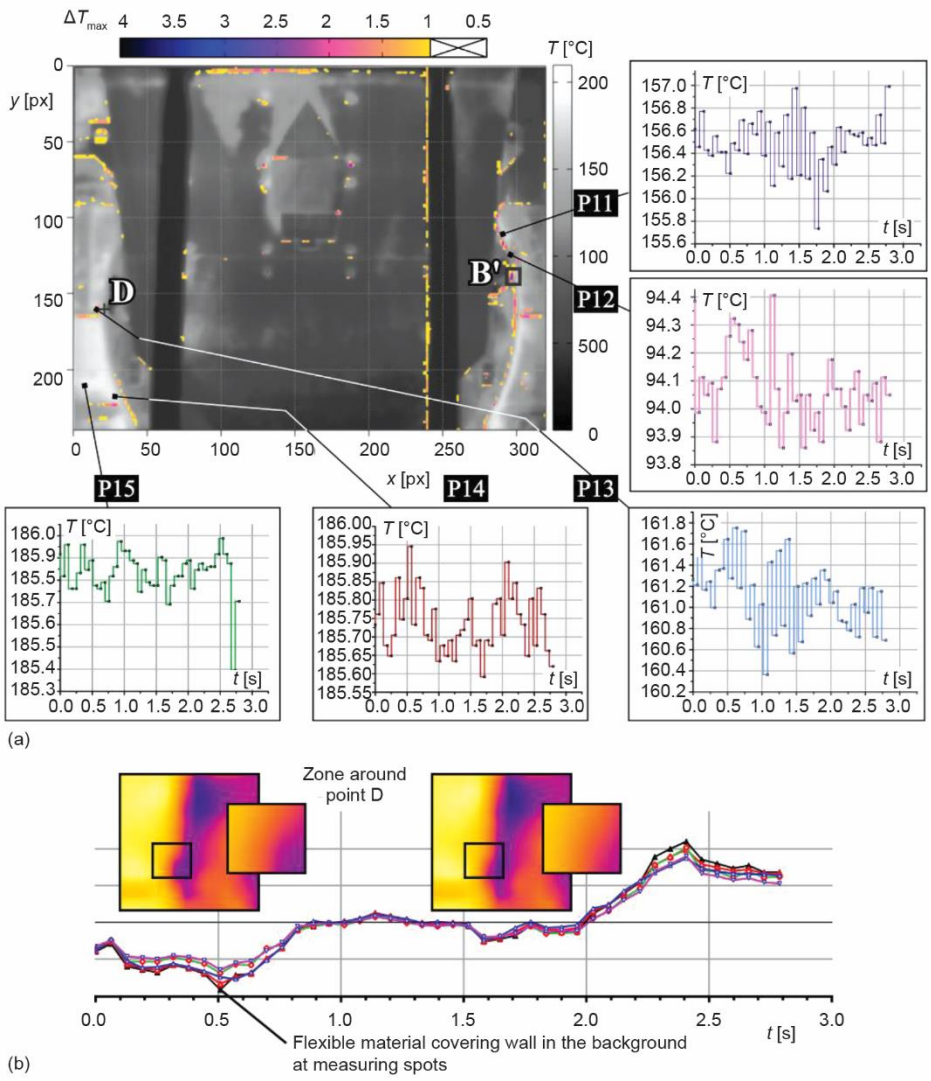

Legend

	No.	x [px]	y [px]	ΔT_{max} [ºC]	T_{max} [ºC]	T_{min} [ºC]	$\bar{T}$ [ºC]
	1(D)	22	156	20.146	87.701	67.555	78.539
	2	22	157	18.216	80.443	62.227	72.11
	3	22	155	17.115	100.379	83.264	93.48
	4	22	158	16.415	73.101	56.686	65.408
	5	22	156	15.482	87.701	67.55	78.539

Figure 6. Combined results from Test 3 (the front side); (a) overlapped maps of T and ΔT_{max} [19] with the diagrams of the $T(t)$ at the points P11-P15 and (b) curves $T'(t)$ at the spots with the five highest ΔT_{max} [19]

results, a research type (high resolution and high speed) thermal camera is recommended since PATS is adapted for use with different thermal cameras, both industrial and research ones. The most important advantages of PATS are shown in its easy implementation, ability to analyze large datasets, and decision making on experiment quality and design just after a test, in the working place, which significantly contributes to the testing cost-effectiveness. The future plans based on the present experiences, are to update PATS to make it more user-friendly.

Conclusion

A combined method of IRT and the PATS software in observations of the free convective flow boundary-layer, used in the case of thermal plant VM walls, shows that the method has potential to be implemented in practice for the recognition of turbulent flow zones. The obtained results, especially those concerning different obstacles with simplified surface topologies, have shown that IRT and PATS are suitable for positioning measurement points for the application of more precise methods (devices); a similar method has not been found reported yet. Although the method requires further development, it has fulfilled its main tasks of decreasing the time needed for implementation, broadening the knowledge base, testing, and decision-making. We hope that the presented investigation will motivate new and more detailed research, contribute to the research in the field of free convective flow, and serve as a supplementary method to the existing ones.

Acknowledgment

This work was financially supported by the Ministry of Education, Science and Technological Development of the Republic of Serbia (Grant No. 451-03-68/2020-14/200026). The authors are also thankful for the support of the following institutions: University of Belgrade, Innovation Center of the Faculty of Mechanical Engineering; University of Belgrade, Institute of Chemistry, Technology, and Metallurgy, IHTM; Goša Institute d.o.o., Belgrade; and TPP "Kostolac", Kostolac, Serbia. For the transfer of knowledge and constructive support to experimental realization, we are thankful to Mirko Kozić, Ph.D., Principal Research Fellow, and Boris Katavić, Ph.D., Senior Research Associate.

Nomenclature

f – frame rate, [fps]
n – number of recorded frames, [–]
T – surface temperature at the spot, [°C]
$\bar{T}$ – time averaged temperature at the spot on the surface, [°C]
T' – fluctuating component of temperature, [°C]
ΔT – temperature peak-to-peak change at the spot, [°C]
t – time of recording, [s]
x – spot coordinate along the abscissa on the image, [px]
y – spot coordinate along the ordinate on the image, [px]

Subscripts

min – minimum value
max – maximum value

References

[1] Lienhard IV, J., Lienhard ,V., J., *A Heat Transfer Textbook*, 3rd ed., Phlogiston Press, Cambridge, Mass., USA, 2008
[2] Cengel, Y. A., *Heat Transfer: A Practical Approach*, 2nd ed., McGraw-Hill, New York, USA, 2002
[3] Jiji, L. M., *Heat Convection*, 2nd ed., Springer, New York, USA, 2009
[4] Martynenko, O. G., *et al*., *Free-Convective Heat Transfer: With Many Photographs of Flows and Heat Exchange*, Springer, New York, USA, 2005
[5] White, F., *Viscous Fluid Flow*, 3rd ed., McGraw-Hill, New York, USA, 2006

[6] Zhao, Y., *et al*., Resonance of the Thermal Boundary Layer Adjacent to an Isothermally Heated Vertical Surface, *J. Fluid Mech., 724* (2013), June, pp. 305-336
[7] Ristić, S., *et al*., Turbulence Investigation in the VTI's Experimental Aerodynamics Laboratory, *Thermal Science, 21* (2017), Suppl. 3, pp. S629-S647
[8] Tsuji, T., Nagano, Y., Velocity and Temperature Measurements in a Natural Convection Boundary Layer Along a Vertical Flat Plate, *Experimental Thermal and Fluid Science, 2* (1989), 2, pp. 208-213
[9] De Larochelambert, T., Transition to Turbulence in Strongly Heated Vertical Natural Convection Boundary Layers, *Proceedings* (Ed. H. C. de Lange and A. A. van Steenhoven, *Heat transfer in unsteady and transitional flows*) EUROTHERM Seminar 74, Eindhoven, The Netherlands, 2003, pp. 183-188, <hal-00347703>
[10] Malerba, M., *et al*., A Boundary Layer Inspection on a Wing Profile Through High Resolution Thermography and Numerical Methods, *WSEAS Transactions on Fluid Mechanics, 3* (2008), 1, pp. 18-28
[11] Montelpare, S., Ricci, R., A Thermographic Method to Evaluate the Local Boundary Layer Separation Phenomena on Aerodynamic Bodies Operating at low Reynolds Number, *International Journal of Thermal Sciences, 43* (2004), 3, pp. 315-329
[12] Simon, B., *et al*., IR-Thermography for Dynamic Detection of Laminar-Turbulent Transition, *Proceedings,* 18th International Symposium on the Application of Laser and Imaging Techniques to Fluid Mechanics, Lisbon, Portugal, 2016
[13] Linić, S., *et al*., Boundary Layer Transition Detection by Thermography and Numerical Method Around Bionic Train Model in Wind Tunnel Test, *Thermal Science, 22* (2018), 2, pp. 1137-1148
[14] Kozić, M., *et al*., Numerical and Experimental Study of Temperature Distribution on Thermal Plant Coal Mill Walls, *Environmental Progress & Sustainable Energy, 36* (2017), 5, pp. 1517-1527
[15] Kozić, M., *et al*., Determination of the Temperature Distribution on the Walls of Ventilation Mill by Numerical Simulation of Multiphase Flow and Thermography, *Proceedings,* 5th International Congress of Serbian Society of Mechanics, The Serbian Society of Mechanics, Arandjelovac, Serbia, 2015, F2c, pp. 1-8
[16] Linić, S., *et al*., One Method for Determining Turbulence Measuring Places Applied to Free-Convection Flow Around Thermal Plant Coal Mill, *Proceedings,*7th International Congress of Serbian Society of Mechanics, Sremski Karlovci, Serbia, 2019, M3G, pp. 1-10
[17] Linić, S., *et al*., *The Investigation of the Temperature Distribution Around the Ventilation Mill with Thermography, the Study – in Serbian*, Project TR34028, Institute Goša d.o.o., Belgrade, pp. 9-34, 2017
[18] Schlichting, H., *Boundary-Layer Theory*, 7th ed., McGraw-Hill, New York, USA, 1979
[19] Linić, M., *The Software for Analyze of the Thermal Video Records – PATS – in Serbian*, Final Work, Electrical Engineering High School "Nikola Tesla", Belgrade, Serbia, 2020
[20] ***, Visual Studio, Microsoft Corp., https:// visualstudio.microsoft.com
[21] Williams, T., *et al*., Gnuplot, http://www.gnuplot.info

Paper submitted: September 7, 2020
Paper revised: October 23, 2020
Paper accepted: October 26, 2020